formation (*10*). We investigated the retinoid-induced RXR homodimer binding to the TREpal by gel retardation assay (*16*). In the absence of 9-*cis*-RA, RXR did not bind to this response element (Fig. 3). Retinoids SR11217 and SR11237 induced RXR homodimer binding to the response element in a concentration-dependent manner. Retinoid SR11203, which behaved as a weak activator in the transient transfection assays, .induced weak RXR binding (*17*), whereas the strongest activators, SR11217 and SR11237, induced homodimer binding very effectively, as judged from the strength of the band induced (Fig. 3). Retinoid SR11231, which did not activate the RXR homodimer (*17*), was not able to induce RXR homodimer binding, either. Similar results were obtained with the CRBPII-RARE and the apolipoprotein AI (apoAI)–RARE (*17*).

To analyze whether these retinoids were selective for RXR homodimers, we used reporter constructs carrying either the rat cytoplasmic retinol-binding protein I (CRBPI) gene RARE (*18*), which is only bound and activated by RAR-RXR heterodimers (*10*); the RARβ2 gene promoter RARE (*19*), which is most effectively bound by heterodimers but also activated to some degree by RXR homodimers (*10*); the CRBPII-RARE, which is activated only by RXR homodimers (*10*) and on which RAR represses RXR activity (*14*, *17*); or the apoAI gene RARE (*20*), which is bound and activated by RAR-RXR heterodimers as well as by RXR homodimers. Each reporter construct was cotransfected with RARα, RARβ, RXRα, or RXRα and RARα together (*13*). The retinoids were analyzed at a concentration of 5×10^{-7} M (a dose shown to yield almost full induction, Fig. 2). The retinoids activated only RXR homodimers, but not RAR-RXR heterodimers (Fig. 4). Like 9-*cis*-RA, both SR11217 and SR11237 were strong activators of the CRBPII-RARE. However, in contrast to 9-*cis*-RA, they did not induce the CRBPI-RARE, which is activated only by the RAR-RXR heterodimer (Fig. 4). Thus, although SR11217 and SR11237 behaved very similarly to 9-*cis*-RA on the CRBPII-RARE, they showed no response on the CRBPI-RARE, on which 9-*cis*-RA is the optimal activator. The βRARE was slightly activated by SR11217 and SR11237, consistent with the relatively low affinity of RXR homodimers for this response element (*10*). The apoAI-RARE was most effectively activated by RAR-RXR heterodimers in the presence of 9-*cis*-RA, as observed previously (*10*). In addition to the activity found in CV-1 cells, a significant and RXR-specific activation by retinoids SR11217 and SR11237 was seen in various other cell lines, including Hep G2 cells, where a high response was seen. When cotransfected alone, RARα, RARβ, and RARγ were not activated significantly by any of the synthetic retinoids on any of the response elements tested (Fig. 4) (*17*). Heterodimers that RARα and RARβ form with endogenous RXR-like proteins in CV-1 cells were also unresponsive to these retinoids.

These retinoids thus specifically induce RXR homodimer formation and activate RXR homodimers, but not RAR-RXR heterodimers. These retinoids allow the specific activation of RXR-selective response pathways but do not induce RAR-dependent response pathways. They should provide a more restricted physiological response than previously available RA isomers and may be useful for elucidation of retinoid response pathways. Pathological conditions and biological pathways that are only affected by pharmacological doses of RA (*21*), where RA may induce RXR homodimer formation (*10*), could also be responsive to this class of retinoids.

REFERENCES AND NOTES

1. W. Bollag, *Lancet* i, 860 (1983); K. H. Kraemer, J. J. Di Giovanna, A. N. Moshell, R. E. Tarone, G. L. Peck, *N. Engl. J. Med.* **318**, 1633 (1988).
2. R. Lotan, *Biochim. Biophys. Acta* **605**, 33 (1981); A. B. Roberts and M. B. Sporn, *The Retinoids*, (Academic Press, New York, 1984), pp. 209–286; S. M. Lippman, J. F. Kessler, F. L. Meyskens, *Cancer Treat. Rep.* **71**, 391 (1987); *ibid.*, p. 493; W. K. Hong *et al.*, *N. Engl. J. Med.* **323**, 795 (1990); M. E. Huang *et al.*, *Blood* **72**, 567 (1988).
3. V. C. Yu *et al.*, *Cell* **67**, 1251 (1991).
4. X.-k. Zhang, B. Hoffmann, P. B.-V. Tran, G. Graupner, M. Pfahl, *Nature* **355**, 441 (1992).
5. M. Leid *et al.*, *Cell* **68**, 377 (1992).
6. S. A. Kliewer, K. Umesono, D. J. Mangelsdorf, R. M. Evans, *Nature* **355**, 446 (1992).
7. T. H. Bugge, J. Pohl, O. Lonnoy, H. G. Stunnenberg, *EMBO J.* **11**, 1409 (1992).
8. M. S. Marks *et al.*, *ibid.*, p. 1419.
9. T. Hermann, B. Hoffmann, X.-k. Zhang, P. Tran, M. Pfahl, *Mol. Endocrinol.* **6**, 1153 (1992).
10. X.-k. Zhang *et al.*, *Nature* **358**, 587 (1992).
11. A. A. Levin *et al.*, *ibid.* **355**, 359 (1992); R. Heyman *et al.*, *Cell* **68**, 397 (1992).
12. G. Graupner, K. N. Wills, M. Tzukerman, X.-k. Zhang, M. Pfahl, *Nature* **340**, 653 (1989); X.-k. Zhang *et al.*, *New Biol.* **3**, 169 (1991).
13. Transient transfections were carried out essentially as described (*4*). M. Husmann *et al.*, *Mol. Cell Biol.* **11**, 4097 (1991).
14. D. J. Mangelsdorf *et al.*, *Cell* **66**, 555 (1991).
15. M. I. Dawson, J. M. Lehmann, M. Pfahl, unpublished results.
16. Gel retardation assays as described previously in X.-k. Zhang *et al.*, *Mol. Endocrinol.* **5**, 1909 (1991).
17. A. Fanjul, X.-P. Lu, J. M. Lehmann, M. I. Dawson, M. Pfahl, unpublished results.
18. M. Husmann, B. Hoffmann, D. G. Stump, F. Chytil, M. Pfahl, *Biochem. Biophys. Res. Commun.* **187**, 1558 (1992).
19. H. de Thé, M. d. M. Vivanco-Ruiz, P. Tiollais, H. Stunnenberg, A. Dejean, *Nature* **343**, 177 (1990); B. Hoffmann *et al.*, *Mol. Endocrinol.* **4**, 1734 (1990).
20. J. N. Rottman, R. L. Widom, B. Nadal-Ginard, V. Mahdavi, S. K. Karathanasis, *Mol. Cell. Biol.* **11**, 3814 (1991).
21. N. Sidell, A. Altman, M. R. Haussler, R. C. Seeger, *Exp. Cell Res.* **148**, 21 (1983); M. K. S. Edwards and M. W. McBurney, *Dev. Biol.* **98**, 187 (1983).

22. We thank E. Adamson and E. Ruoslahti for comments on the manuscript and X.-k. Zhang for discussions. Supported by National Cancer Institute grants P01 CA51993 (M.I.D.) and CA50676 (M.P.).

2 September 1992; accepted 23 October 1992

Isolation and Structure of a Brain Constituent That Binds to the Cannabinoid Receptor

William A. Devane,*† Lumir Hanuš, Aviva Breuer, Roger G. Pertwee, Lesley A. Stevenson, Graeme Griffin, Dan Gibson, Asher Mandelbaum, Alexander Etinger, Raphael Mechoulam†

Arachidonylethanolamide, an arachidonic acid derivative in porcine brain, was identified in a screen for endogenous ligands for the cannabinoid receptor. The structure of this compound, which has been named "anandamide," was determined by mass spectrometry and nuclear magnetic resonance spectroscopy and was confirmed by synthesis. Anandamide inhibited the specific binding of a radiolabeled cannabinoid probe to synaptosomal membranes in a manner typical of competitive ligands and produced a concentration-dependent inhibition of the electrically evoked twitch response of the mouse vas deferens, a characteristic effect of psychotropic cannabinoids. These properties suggest that anandamide may function as a natural ligand for the cannabinoid receptor.

The psychoactive constituent of cannabis, Δ^9-tetrahydrocannabinol (Δ^9-THC) (*1*), binds to a specific G protein–coupled receptor in the brain (*2*). Sequence information on the cannabinoid receptor is available from cloned rat (*3*) and human (*4*) genes, but thus far it has not provided insight into the protein's physiological role(s). The abundance and anatomical localization of the receptor in the brain (*5*), together with the behavioral effects of Δ^9-THC (*6*), are consistent with roles in the control of

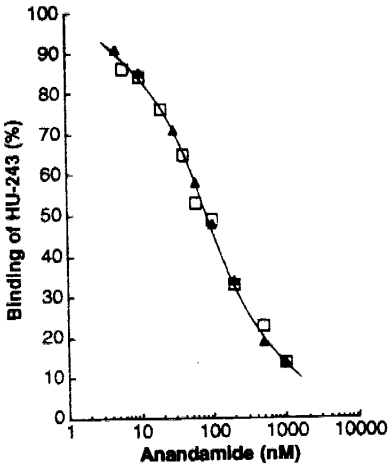

Fig. 1. Competitive inhibition of [^{3}H]HU-243 binding by natural anandamide. Synaptosomal membranes were prepared from the brains of Sprague-Dawley male rats (430 to 470 g) after removal of the brainstem. The [^{3}H]HU-243 probe (45 to 55 pM) was incubated with synaptosomal membranes (3 to 4 μg) for 90 min at 30°C with the indicated concentrations of anandamide or with the vehicle alone (fatty-acid–free bovine serum albumin at a final concentration of 0.5 mg/ml). Bound and free radioligand were separated by centrifugation [see (*8*) for full details of the assay]. The data were normalized to 100% of specific binding, which was determined with 50 nM unlabeled HU-243. Specific binding accounted for 77 to 82% of the total radioactivity bound to the membranes. Data points represent the average of triplicate determinations from two independent experiments. The K_i value was determined from the Ligand program (*26*).

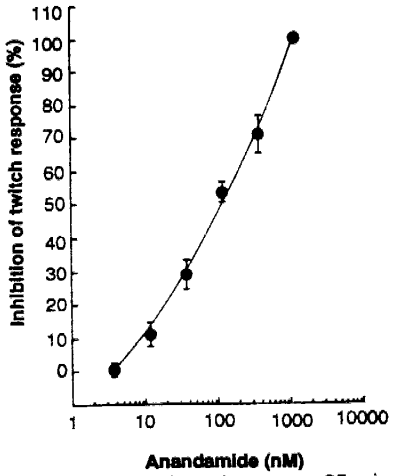

Fig. 2. Inhibition of the vas deferens twitch response by natural anandamide. Data are presented as the percentage of inhibition ± SEM (n = 6 or 7) for each concentration. Vas deferentia from MF1 mice were mounted in siliconized organ baths (4 ml) under an initial tension of 0.5 g. The baths contained Mg^{2+}-free Krebs solution (*13*), which was kept at 37°C and bubbled with 95% O_2 and 5% CO_2. The tissues were stimulated supramaximally with 0.5-s trains of three pulses (train frequency, 0.1 Hz; pulse duration, 0.5 ms). Isometric contractions were evoked by electrical field stimulation through electrodes attached at the upper and lower ends of each bath and were registered on a polygraph recorder (Grass model 7D) with Pye Ether UF1 transducers. The effect of natural anandamide on the twitch response was measured 30 min after its administration. As in previous experiments with cannabinoids (*13*), only one dose was added to each tissue and a pattern of intermittent stimulation was used. Each tissue was subjected to an 11-min period of stimulation, then to a 25-min stimulation-free period, and finally to a second, 5-min period of stimulation. Natural anandamide was added in a volume of 40 μl at the end of the first 11-min period of stimulation. The anandamide was dispersed in Tween-80 and saline (*13*). Tween-80 alone did not inhibit the twitch response (n = 6) at the maximum concentration used in the baths (0.63 μg/ml).

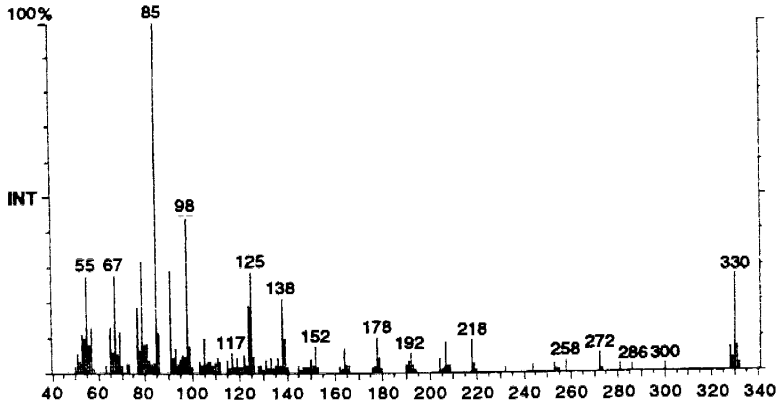

Fig. 3. GC-MS spectrum of anandamide in an ion-trap instrument [for details, see (*12*)]. Anandamide undergoes thermal dehydration under these conditions; hence the spectrum shown is that of the $M^{+\cdot}$ ion of the corresponding 2-oxazoline.

movement, memory, emotions, and pain modulation, among other activities. Although a specific endogenous ligand for the cannabinoid receptor has not yet been identified, its existence is predicted from the strict structural requirements for receptor activation by exogenous ligands (*7*). Moreover, the 97.3% sequence conservation displayed by the rat and human cannabinoid receptors (*4*) suggests that this endogenous ligand(s) may also be conserved across species.

To screen for endogenous cannabinoid compounds, we tested the ability of fractions from porcine brain extracts to displace a radiolabeled cannabinoid probe in a centrifugation-based ligand binding assay. The probe, [^{3}H]HU-243 (11-hydroxy-hexahydrocannabinol-3-dimethylheptyl homolog), has a dissociation constant of 45 pM in rat synaptosomal membranes (*8*). Organic solvent extracts of porcine brain were first chromatographed according to standard protocols for the separation of lipids (*9*). Because many of the initial fractions inhibited the binding of [^{3}H]HU-243 to the cannabinoid receptor, we paid particular attention to the binding of [^{3}H]HU-243 to the siliconized polypropylene microfuge tubes in which the assay was conducted. Normally, about 15 to 20% of the added [^{3}H]HU-243 adheres to the microfuge tube, with the amount increasing slightly when unlabeled cannabinoid drugs displace the radioligand from the receptor. When monitoring the three-way equilibrium of [^{3}H]HU-243 among the synaptosomal receptors, the solution, and the microfuge tube, we observed that all the crude brain fractions that inhibited the binding of [^{3}H]HU-243 to the receptors also inhibited the binding of the radioligand to the microfuge tube. We speculated that these fractions contained compounds that sequestered the radioligand in the solution, perhaps in micelles formed by lipids. After analyzing the binding behavior of [^{3}H]HU-243 at different concentrations of the brain fractions, we chose those fractions that inhibited binding to the receptor but had the least effect on the adherence of the radioligand to the microfuge tube. Several promising fractions were further purified by low- and medium-pressure column chromatography and by thin-layer chromatography (TLC). Both normal-phase and reversed-phase systems were used (*10*).

From these fractions we purified a compound (final yield = 0.6 mg from 4.5 kg of brain) that we named anandamide (*11*). Anandamide showed one spot on TLC and eluted as one main peak on gas chromatography (GC) when a mass spectrometer was used as a detector (*12*). Anandamide inhibited the specific binding of [^{3}H]HU-243 to

W. A. Devane, L. Hanuš, A. Breuer, D. Gibson, R. Mechoulam, Department of Natural Products, Medical Faculty, Hebrew University, Jerusalem 91120, Israel.
R. G. Pertwee, L. A. Stevenson, G. Griffin, Department of Biomedical Sciences, Marischal College, University of Aberdeen, Aberdeen AB9 1AS, United Kingdom.
A. Mandelbaum and A. Etinger, Department of Chemistry, Technion–Israel Institute of Technology, Haifa 32000, Israel.

*Present address: Laboratory of Cell Biology, National Institute of Mental Health, Building 36, Room 3A-15, Bethesda, MD 20892.
†To whom correspondence should be addressed.

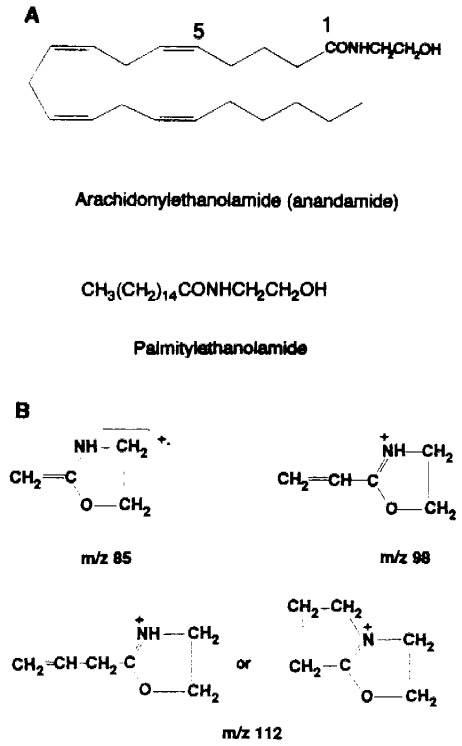

Fig. 4. Structures of anandamide and palmitylethanolamide (**A**) and the dihydro- and tetrahydrooxazole ion fragments (**B**) formed from these compounds on thermal dehydration under GC-MS conditions. The *m/z* 112 ion is formed only from palmitylethanolamide.

synaptosomal membranes in a manner typical of competitive ligands (8), with an inhibition constant (K_i) value (± standard error of the mean; n = 3) of 52 ± 1.8 nM (Fig. 1). In this system, the K_i of Δ^9-THC was 46 ± 3 nM (8).

To determine whether anandamide had cannabimimetic pharmacological activity, we investigated its ability to inhibit the twitch response of isolated murine vas deferentia. This assay was chosen because previous studies had shown it to be a suitable and sensitive model for investigating the mode(s) of action of psychotropic cannabinoids (13). Anandamide produced a concentration-dependent inhibition of the twitch response, decreasing twitch heights by 50% at a concentration of 90 nM (Fig. 2). The inhibition was not reversed by addition of the opioid antagonist naloxone at a concentration of 300 nM. Both the potency of anandamide and the degree of inhibition it produced in this functional assay were comparable to those observed in the receptor binding assay. However, like other bioassays for cannabinoids, the mouse vas deferens assay lacks specificity. Thus, although the naloxone experiment indicated that anandamide did not exert its inhibitory effect on the vas deferens through opioid receptors, we cannot firmly conclude that the inhibition was mediated through the cannabinoid receptor.

The structure of anandamide was established by mass spectrometry (MS) and nuclear magnetic resonance (NMR) spectroscopy. A variety of MS measurements were performed on the purified material (12). Direct-exposure chemical ionization (isobutane-DCI) mass spectrum indicated a molecular weight of 347 (*m/z* 348 MH^+ ion). High-resolution MS measurements suggested the elemental composition $C_{22}H_{37}NO_2$ (*m/z* 347.2762), which is consistent with the presence of five double bonds or rings. Collision-induced dissociation (CID) measurements of the *m/z* 348 MH^+ ion (obtained under isobutane-DCI) gave rise to the following significant fragments: *m/z* 287, 245, 203, 62 (highest abundance), and 44. The only reasonable composition of the most abundant *m/z* 62 fragment ion is C_2H_8NO, which corresponds to protonated ethanolamine $HOCH_2CH_2NH_3^+$. The *m/z* 44 ion may be formed by dehydration of the *m/z* 62 fragment. The *m/z* 287 $[MH\text{-}61]^+$ fragment ion corresponds to the loss of ethanolamine (C_2H_7NO) from MH^+. Additional data were obtained from the GC-MS and CID measurements of the trimethylsilyl (TMS) derivative of the purified material (14). Together, these results suggested that anandamide is an ethanolamide of a tetraenic C_{20} fatty acid.

Supporting evidence for this general structure was found in the behavior of anandamide under GC-MS conditions (12). Thermal dehydration gave rise to *m/z* 329 $M^{+\cdot}$ ion upon electron ionization (EI) and to *m/z* 330 MH^+ ion under CI. Both self-CI *m/z* 330 MH^+ and *m/z* 329 $M^{+\cdot}$ were formed under EI conditions in an ion-trap instrument (12) (Fig. 3). A similar dehydration under GC-MS conditions was also observed for synthetic palmitylethanolamide (15), and it presumably leads to the formation of 2-oxazoline derivatives (16). The fragmentation patterns of the dehydration products of anandamide and palmitylethanolamide were similar in the low mass range of the EI mass spectra and included *m/z* 85 (McLafferty rearrangement ion) and *m/z* 98 (product of a γ-cleavage) (Fig. 4). The EI mass spectrum of dehydrated palmitylethanolamide exhibited an *m/z* 112 ion that corresponded to a δ-cleavage fragment. The absence of this ion from the EI mass spectrum obtained in the GC-MS analysis of anandamide suggests the presence of the first double bond in the tetraenic acid at position 5 (as in arachidonylethanolamide, which would not be expected to yield a δ-cleavage product) (Fig. 4).

Because of the small amount of natural anandamide available, we were able to record ^1H NMR spectra only (17). The peaks attributed to double-bond protons (δ 5.30 to 5.45, multiplet) were coupled with those of protons that have the chemical shifts of doubly allylic protons (δ 2.75 to 2.90, multiplet). Such doubly allylic protons are typically found in all-*cis*, nonconjugated polyunsaturated fatty acids such as linoleic and arachidonic acids (18). Three pairs of protons were observed between δ 2.01 and 2.27, which we attributed to two allylic methylene groups and one methylene group α to a carbonyl moiety. Only one methyl group was observed [0.88, t (triplet)]. The peaks observed for two protons at 3.42 (N-CH_2, t), two protons at 3.72 (O-CH_2, t), and two protons at 2.20 ($COCH_2$, t) were similar in chemical shifts and spin-coupling patterns to peaks observed in the NMR spectrum of synthetic palmitylethanolamide. The peaks for N-CH_2 and O-CH_2 were coupled.

A juxtaposition of the various analytical data led us to conclude that the structure of anandamide is that of arachidonyl ethanolamide [5,8,11,14-eicosatetraenamide,(*N*-2-hydroxyethyl)-(all-Z)]. This conclusion was confirmed by synthesis (19). Synthetic arachidonylethanolamide was identical with the natural product on TLC, NMR (300 MHz), and GC-MS (retention time and fragmentation pattern) (Fig. 3). Synthetic anandamide bound to the cannabinoid receptor with a K_i of 39 ± 5.0 nM (n = 3).

Classification of a substance as a neuromediator requires fulfillment of numerous criteria, such as receptor specificity and appropriate cellular localization. Although our present results, therefore, do not establish that anandamide is a neuromediator, it is noteworthy that three related lipids, palmitylethanolamide, arachidonic acid methyl ester, and phytanic acid, did not inhibit the binding of [^3H]HU-243 to the cannabinoid receptor in concentrations up to 1 μM (15). Howlett *et al.* (20) have investigated the effect of 136 natural and synthetic ligands for various receptors, including 24 eicosanoid derivatives, on binding of the cannabinoid probe [^3H]CP-55940 to rat brain membranes, with essentially negative results. These observations indicate that binding to the cannabinoid receptor by vertebrate constituents is thus far limited to anandamide. We have, however, detected additional porcine brain constituents that display cannabinoid-like activity in both the binding and the vas deferens assays. These constituents appear to differ from anandamide in potency, efficacy, and rate of onset of action (15).

The identification of anandamide as a potential ligand for the cannabinoid receptor reaffirms the biological importance of fatty acid amides and their derivatives. In 1957, palmitylethanolamide from egg yolk was shown to be an anti-inflammatory agent (21), and, in 1965, fatty acid amides of ethanolamine were shown to be endogenous products of mammalian brain tissue

22). More recently, a fatty acid amide isolated from bovine mesentery was found to be angiogenic (23), and synthetic arachidonamide was found to inhibit leukotriene biosynthesis (24). Our results raise the possibility that anandamide is formed via an as-yet-uncharacterized route of arachidonic acid metabolism leading to compounds that act, at least in part, through the cannabinoid receptor.

Finally, our results may help to clarify the biological significance of previously reported interactions between cannabinoids and eicosanoids (25).

REFERENCES AND NOTES

1. Y. Gaoni and R. Mechoulam, *J. Am. Chem. Soc.* **86**, 1646 (1964).
2. W. A. Devane, F. A. Dysarz III, M. R. Johnson, L. S. Melvin, A. C. Howlett, *Mol. Pharmacol.* **34**, 605 (1988); W. A. Devane, thesis, St. Louis University, St. Louis, MO, (1989).
3. L. A. Matsuda, S. J. Lolait, M. J. Brownstein, A. C. Young, T. I. Bonner, *Nature* **346**, 561 (1990).
4. C. M. Gérard, C. Mollereau, G. Vassart, M. Parmentier, *Biochem. J.* **279**, 129 (1991).
5. M. Herkenham *et al.*, *Proc. Natl. Acad. Sci. U.S.A.* **87**, 1932 (1990); M. Herkenham *et al.*, *J. Neurosci.* **11**, 563 (1991).
6. R. G. Pertwee, *Pharmacol. Ther.* **36**, 189 (1988).
7. R. Mechoulam *et al.*, *Experientia* **44**, 762 (1988); R. Mechoulam, W. A. Devane, R. Glaser, in *Marijuana/Cannabinoids: Neurobiology and Neurophysiology*, L. Murphy and A. Bartke, Eds. (CRC Press, Boca Raton, FL, 1992), pp. 1–33.
8. W. A. Devane *et al.*, *J. Med. Chem.* **35**, 2065 (1992).
9. Porcine brains were homogenized in chloroform and/or methanol and centrifuged at 13,000*g*. The organic solvent extract was fractionated over a silica column (70 to 230 μm, Kieselgel 60, Merck), according to elution schemes used to separate the major classes of lipids [C. C. Sweeley, *Methods Enzymol.* **14**, 254 (1969); J. C. Dittmer and M. A. Wells, *ibid.*, p. 482].
10. The TLC plates (analytical, RP-18, Merck) were eluted with methanol-dichloromethane (4:1) and developed twice. The first solvent front was at 3.1 cm, and the second was at 7.4 cm. The R_f value was 0.65 [W. A. Devane, L. Hanuš, R. Mechoulam, *Proceedings of the Fifth Nordic Neuroscience Meeting*, Publ. Univ. Kuopio Med. (1991), p. 198]. Anandamide eluted from a silica column (Kieselgel 60, 40 to 63 μm, Merck) with methanol-chloroform (2:98). It eluted from a reversed-phase column (RP-C_{18}, 40 to 63 μm, Sigma) with methanol-water (88:12).
11. The term "anandamide" was coined from the Sanskrit word "ananda," meaning bliss, and from the chemical nature of the compound.
12. GC-MS analyses were carried out with a Finnigan ITS-40 system and with a Finnigan TSQ-70B triple-stage quadrupole mass spectrometer coupled to a Varian 3400 gas chromatograph. Separations were performed on a DB-5 (0.25-μm film) capillary column that was 30 m in length and had an internal diameter (i.d.) of 0.25 mm. The column temperature was programmed to increase from 60 to 280°C at a rate of 20°C per minute. The compounds were injected into the GC in methylene chloride. The electron energy in EI measurements was 70 eV with one scan per second. The isobutane DCI measurements were carried out with a TSQ-70B mass spectrometer under standard conditions. High-resolution mass spectral measurements were performed with a Varian-MAT 711 double-focusing mass spectrometer. The CID measurements were carried out with the TSQ-70B triple-stage mass spectrometer. The collision energy was 50 eV, and argon was used as the target gas at an indicated pressure of 0.4 mtorr.
13. R. G. Pertwee, L. A. Stevenson, D. B. Elrick, R. Mechoulam, A. D. Corbett, *Br. J. Pharmacol.* **105**, 980 (1992).
14. The GC-MS and CID measurements of the TMS derivative of anandamide gave m/z 419 M^+ and 404 $[M\text{-}CH_3]^+$ fragment ions, which indicated formation of a mono-TMS ether. The CID spectrum of the m/z 404 ion exhibited two major fragment ions at m/z 118 and 172, corresponding to $Me_2Si^+OCH_2CH_2NH_2$ and $Me_2Si^+OCH_2CH_2NHCOCH{=}CH_2$, respectively.
15. W. A. Devane *et al.*, unpublished data.
16. H. Wenker, *J. Am. Chem. Soc.* **57**, 1079 (1935).
17. The one- and two-dimensional proton NMR spectra (in $CDCl_3$) were obtained on a Varian VXR300s spectrometer equipped with a 5-mm computer switchable probehead and on an AMX 400.133 Bruker spectrometer with a 5-mm reverse probehead. The chemical shifts are presented in parts per million. The Bruker library program (NOESY) was used for the two-dimensional measurements.
18. W. W. Christie, *Lipid Analysis* (Pergamon, Oxford, ed. 2, 1982), pp. 81–82; D. J. Frost and J. Barzilay, *Anal. Chem.* **43**, 1316 (1971).
19. Arachidonyl chloride, which was prepared from arachidonic acid and oxalyl chloride according to a published procedure (*24*), was dissolved in methylene chloride and added at 0°C under a nitrogen atmosphere to ethanolamine. The ethanolamine was present in a tenfold molar excess and was also dissolved in methylene chloride. After 15 min the reaction mixture was washed with water, dried, and the product purified by silica column chromatography (eluted with 2% methanol in chloroform) to give arachidonylethanolamide (an oil, ~90% yield) that was 97% pure as judged by GC-MS.
20. A. C. Howlett, D. M. Evans, D. B. Houston, in *Marijuana/Cannabinoids: Neurobiology and Neurophysiology*, L. Murphy and A. Bartke, Eds. (CRC Press, Boca Raton, FL, 1992), pp. 35–72.
21. F. A. Kuehl, Jr., T. A. Jacob, O. H. Ganley, R. E. Osmond, M. A. P. Meisinger, *J. Am. Chem. Soc.* **79**, 5577 (1957).
22. N. R. Bachur, K. Masek, K. L. Melmon, S. Udenfriend, *J. Biol. Chem.* **240**, 1019 (1965).
23. K. Wakamatsu, T. Masaki, F. Itoh, K. Kondo, K. Sudo, *Biochem. Biophys. Res. Commun.* **168**, 423 (1990).
24. E. J. Corey, J. R. Cashman, S. S. Kantner, S. W. Wright, *J. Am. Chem. Soc.* **106**, 1503 (1984).
25. S. H. Burstein, in (*20*), pp. 73–91 and references therein; R. G. Pertwee, *ibid.*, pp. 165–218; J. W. Fairbairn and J. T. Pickens, *Br. J. Pharmacol.* **72**, 401 (1981); A. Sklenovsky, J. Navratil, Z. Chmela, Z. Krejči, L. Hanuš, *Acta Univ. Palacki. Olomuc. Fac. Med.* **122**, 83 (1989).
26. P. J. Munson and D. Rodbard, *Anal. Biochem.* **107**, 220 (1980).

27. Supported by grants to R.M. from the National Institute for Drug Abuse (DA 6481) and the Amdursky Fund of the Friends of the Hebrew University and by a grant to R.G.P. from the Wellcome Trust. We thank I. Ringel (Jerusalem) for the initial NMR work, S. Levin (Jerusalem) for advice on chromatography, and J. Katzir and A. Idina (Haifa) for dedicated technical help.

1 September 1992; accepted 6 November 1992

Direct Visualization of the Dendritic and Receptive Fields of Directionally Selective Retinal Ganglion Cells

Guang Yang and Richard H. Masland*

Optical methods were used to locate the cell bodies of directionally selective ganglion cells in isolated rabbit retinas. These neurons detect the direction in which images move across the retinal surface and transmit that information to the brain. The receptive field of each identified cell was determined, after which the cell was injected with Lucifer yellow. An image of the receptive field border was then projected onto the fluorescent image of the dendrites, allowing precise comparison between them. The size of the receptive field matched closely the size of the dendritic arbor of that cell. This result restricts the types of convergence that can be postulated in modeling the mechanism of retinal directional selectivity.

A classic problem in the study of neural microcircuitry and neural computation is the mechanism by which directionally selective (DS) ganglion cells interpret inputs from preceding retinal neurons to deduce the direction of movement of a visual image formed on the retina (*1–3*). The relatively simple neural circuitry involved and the specific and clear function performed by DS cells have made this problem attractive for computational modeling. However, the modeling has been based on sparse biological facts. The input-output relations of the DS cells have been studied in detail and their dendritic morphology has been established (*4*), but the neural circuits that converge on the DS cells to create directional selectivity are unknown.

Cholinergic inputs from the starburst amacrine cells monosynaptically excite the DS ganglion cells (*5, 6*). The starburst amacrine cells have widely spreading dendritic fields, which overlap extensively (*7*). Because a DS cell receives inputs from many starburst amacrine cells, the receptive field of each DS cell should cover an area considerably wider than the dendritic arbor

Program in Neuroscience and the Department of Neurosurgery, Harvard Medical School, Massachusetts General Hospital, Boston, MA 02114.

*To whom correspondence should be addressed.